

# A Low-Noise CMOS Preamplifier Operating at 4.2 K

U. Kleine, *Member, IEEE*, J. Bieger, and H. Seifert

**Abstract**—A low-noise CMOS readout preamplifier operating at liquid helium temperatures is described. In conjunction with magnetic field sensors applying SQUIDS (Superconducting Quantum Interference Device) the preamplifier can be used to measure biomagnetic fields of human brain and heart non-invasively. The input of the folded cascode amplifier can be attached directly to a low impedance SQUID output. This way the commonly used discrete LC tank resonator circuit for impedance matching can be omitted. An equivalent noise voltage density of 0.3 nV/ $\sqrt{\text{Hz}}$  at 500 kHz has been measured. Despite the occurrence of the kink effect and other abnormalities in MOS transistor characteristics at 4.2 K, during the tests no abnormal operation has been observed. Such a preamplifier circuit is essential in simplifying the expensive shielding currently used in biomagnetic diagnosis systems.

## I. INTRODUCTION

IN recent years, clinical relevance of biomagnetism has been studied extensively. In particular, noninvasive measurement of the magnetic field distributions of the human brain (magneto-encephalograms) and heart (magnetocardiograms) to localize electrical activities have been investigated. For this purpose it is necessary to map the biomagnetic field distribution in a short period of time. This can only be done incorporating a large number of magnetic sensors to form a multichannel system. In 1988, a first operating multichannel system for this purpose was developed at Siemens [1]. Since 1989 [2] the KRENKON®-system employs 37 DC-SQUID's as magnetic flux detectors [3], and additional flux transformers which get their signals from a first order gradiometer array [1], [2]. In order to be able to measure human brain activities, the field resolution needed for the diagnosis system is about 20 fT/ $\sqrt{\text{Hz}}$ . Besides the use of gradiometer pick-up coils to reduce the effect of external noise sources, a special multishell cabin made of soft magnetic walls served to suppress magnetic noise in the frequency range from 1 Hz up to several hundred Hz. Today only liquid helium cooled SQUID sensors can reach the required resolution.

Particularly for applications involving gradiometer arrays, the DC-SQUID [3], [4] is the most suitable sensor device. A symmetrical DC-SQUID consists of a superconducting ring with two identical Josephson junctions (see Fig. 1(a)). The DC-SQUID can be operated by measuring either the average voltage  $V$ , as a function of the external magnetic flux  $\Phi_{\text{ext}}$  with a constant bias current  $I$ , or by measuring the average current with a constant bias voltage. Here a constant

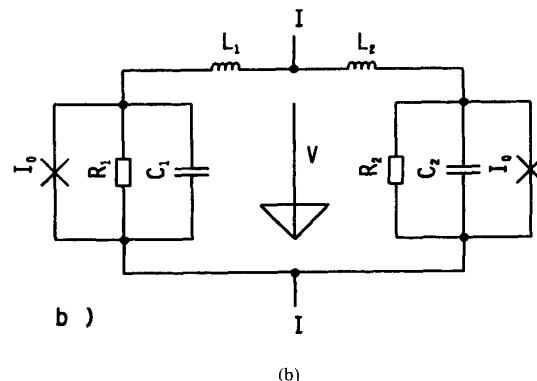
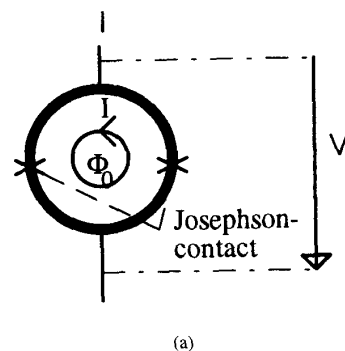


Fig. 1. Symmetrical DC-SQUID: a) Principle arrangement of a DC-SQUID, b) equivalent circuit diagram of a DC-SQUID.

bias current  $I$  is supposed. Fig. 1(b) shows the equivalent circuit diagram.  $L_1$  and  $L_2$  are the loop or ring inductances.  $R_1, R_2$  and  $C_1, C_2$  are respectively the parasitic resistances and junction capacitances of the two Josephson contacts, which are characterized by the critical current  $I_0$  [5]. The resistors are responsible for the thermal noise of the DC-SQUID. Due to the two Josephson contacts, an oscillation in the gigahertz range occurs [3], [5]. The macroscopic superconducting state of the ring is characterized by the phase differences  $\Theta_i$ . If the bias current is smaller than the critical current  $I_0$ , no dc voltage occurs at the terminal of the SQUID. In the normal sensor operation mode ( $I > \text{critical current } 2I_0$ ) a dc voltage  $V$  dependent on the bias current  $I$  occurs at the external nodes. When an external magnetic flux  $\Phi_e$  is coupled into the superconducting ring, a compensation current is induced in the ring. If the bias current  $I$  is kept constant, a periodical voltage-flux-characteristic can be measured. The period of this characteristic is one flux quant  $\Phi_0 = 2.07 \cdot 10^{-15} \text{ Wb}$ . Fig. 2(a)

Manuscript received December 26, 1993; revised March 29, 1994.

U. Kleine is with Siemens AG, Corporate Research and Development, 81370 Munich, Germany.

J. Bieger and H. Seifert are with Siemens Medical Engineering Group, 91052 Erlangen, Germany.

IEEE Log Number 9402469.

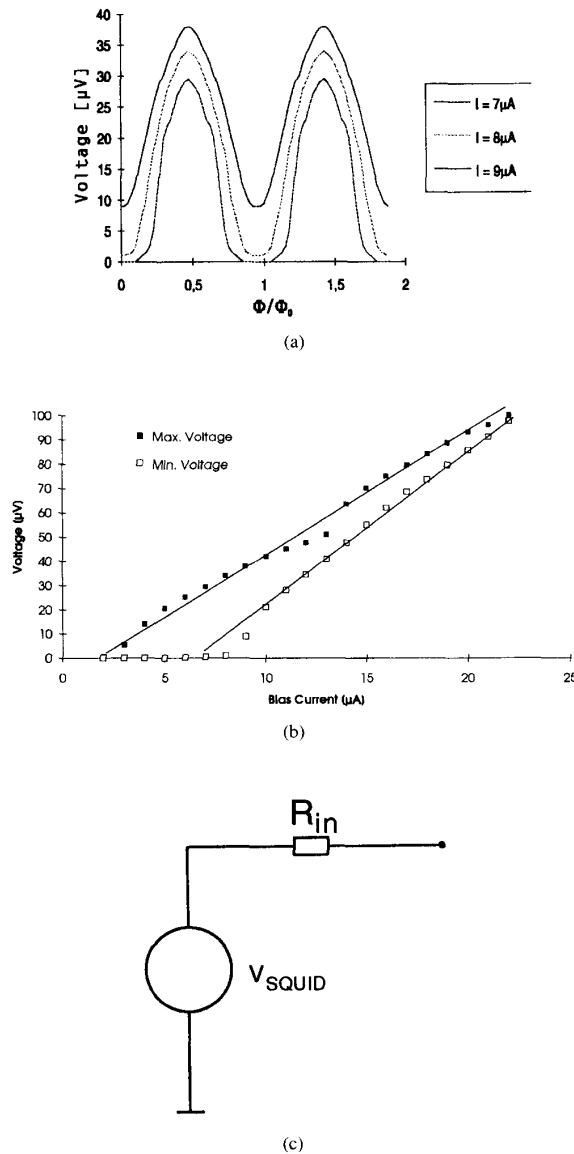


Fig. 2. Principle flux-voltage characteristic of a DC-SQUID: a) Flux-voltage characteristic of a SQUID, b) current-voltage characteristic of a SQUID, c) equivalent circuit diagram.

shows the flux-voltage characteristic for three different bias current settings.

Thus, in order to measure even flux changes smaller than one flux quant, a flux locked loop has to be built around the SQUID. Fig. 3 shows a simplified block diagram of the flux locked loop [1]. The SQUID is modulated with an additional rectangular or sinusoidal signal with an amplitude of  $\Phi_0/2$ . The preamplifier outside the dewar gets its input signal from a LC series resonant tank circuit. As demonstrated in [6], the use of a resonant tank for impedance matching compared to broadband matching using transformers resulted in an improved resolution. The preamplified signal is demodulated,

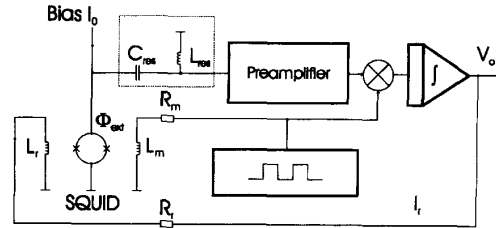


Fig. 3. Block diagram of the flux locked loop.

further amplified, filtered and fed back to the SQUID and to the external signal processing hardware. At a modulation frequency of 100 kHz, the  $1/f$  noise of the SQUID's and the preamplifier is low enough to obtain the required signal to noise ratio.

The feedback electronic can lock the intrinsic flux at any multiple of  $\Phi_0$ . However, an external flux signal should not be able to force the SQUID from one operation point to another. To prevent such a malfunction, the system includes gradiometer coils, which suppress external noise sources approximately by a factor 100, and an expensive shielding cabin [1], [2]. The shielding cabin consists of two layers of Mumetal and one layer of aluminium [2] and suppresses magnetical noise signals from outside the cabin by a factor 1000 above 1 Hz.

One way to reduce the system costs is to simplify the shielding. A precondition for reducing the shielding is an enlarged bandwidth of the flux locked loop to prevent it from locking in a false SQUID operation point. In particular, this can be accomplished by removing the narrow-band resonant tank and substituting the preamplifier by a cooled one closer to the SQUID with high slew-rate, large bandwidth and sufficiently low equivalent input noise.

In this paper a CMOS preamplifier circuit operating at 4.2 K is described which permits the aforementioned saving. In Section II the measurement setup of the amplifier is described, and in Section III the CMOS device characteristics at 4 K are briefly reviewed. Section IV describes the preamplifier circuit, which may be directly connected to the SQUID. Finally, measurement results and some concluding remarks are given in Sections V and VI.

## II. SIMPLIFIED SQUID MODEL AND MEASUREMENT SETUP

In this section the equivalent output resistance of a DC-SQUID is derived. Fig. 2(a) shows the periodic behavior of the voltage  $V$  as a function of the flux  $\Phi$ . The current  $I$  is included in the figure as a third parameter. From Fig. 2(a) a corresponding diagram (see Fig. 2(b)) can be constructed showing the voltage as a function of the current. The maximum voltage values correspond to the peak voltages of the periodic characteristic of the different bias currents (Fig. 2(a)) and the minimum voltage values correspond to the valleys. As can be seen from Fig. 2(b), the output resistance varies between 4 and 10  $\Omega$ . The equivalent circuit diagram of the DC-SQUID is shown in Fig. 2(c). This circuit has been used for modeling the noise behavior.

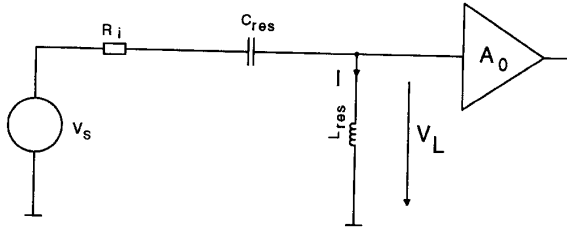


Fig. 4. Impedance matching with a resonance tank circuit.

Since the output impedance of a DC-SQUID is only a few ohms, a transformer is required to match it optimally to the input impedance of several kilohms for bipolar preamplifier or several megohms for a JFET amplifier. Another way to increase the low output impedance is to feed the signal through a capacitor and an inductor set in parallel with the amplifier input (see Fig. 3) [6]. Fig. 4 shows the principle arrangement for the impedance conversion in more detail. With the quality factor  $Q$  being

$$Q = \frac{\omega_{\text{res}} L_{\text{res}}}{R_i}, \quad (1)$$

and by neglecting the input impedance of the amplifier at the resonance frequency  $\omega_{\text{res}}$ , the following equations hold

$$I = \frac{V}{R_{\text{in}}}$$

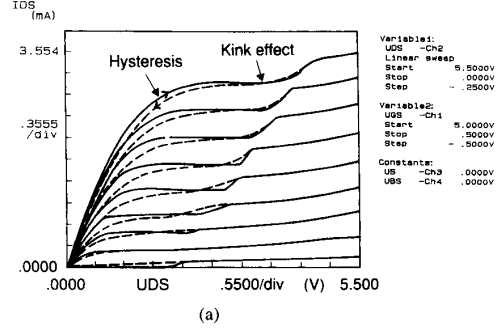
$$V_L = I \omega_{\text{res}} L_{\text{res}} = V \frac{\omega_{\text{res}} L_{\text{res}}}{R_{\text{in}}} = QV. \quad (2)$$

At the resonance frequency a voltage gain of  $Q$  (for this class of applications typically being in the range of 10 to 40) is obtained. In this way the same transformation factor as for the transformer circuit can be achieved. However, (2) holds only at the resonance frequency and therefore, the signal bandwidth is substantially reduced. A direct coupling of the SQUID to the amplifier would solve the bandwidth problem [7], but as the SQUID signal is not amplified noiselessly, as in the case of the passive resonance tank circuit, the noise requirement for the preamplifier is increased. The voltage noise of the preamplifier  $\sqrt{S_V}$  divided by the voltage-flux transfer function  $\delta V / \delta \Phi$  has to be smaller than the magnetic flux noise  $\sqrt{S_B}$ , for which a typical value in the white noise region is  $10^{-5} \Phi_0 / \sqrt{\text{Hz}}$ .

### III. MOS TRANSISTOR CHARACTERISTICS AT 4 K

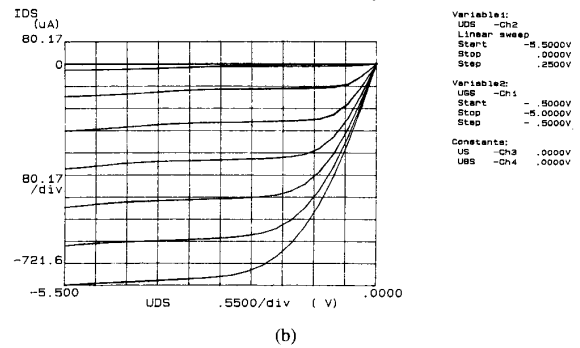
Cryogenic operation at 4.2 K of analog CMOS devices is limited to specific applications, such as infrared applications or low temperature measurements in physical science. Another application is the use of a cooled preamplifier to achieve the low noise requirements in a flux locked loop for a biomagnetical diagnosis system described above. Before starting with the actual preamplifier design, the electrical parameters of the available process had to be studied. Fig. 5 shows the current-voltage characteristics of n- and p-channel MOS transistors at 4.2 K for an analog p-well CMOS technology with 1- $\mu\text{m}$  minimum feature size. As can be seen in the figure, the characteristics exhibit an anomalous behavior [8]–[10]. Kink

#### Current-Voltage Characteristic of an n-MOS Transistor



(a)

#### Current-Voltage Characteristic of an p-MOS Transistor



(b)

 Fig. 5. Current-voltage characteristics of MOS transistors with a  $W/L$  ratio of  $10 \mu\text{m}/3 \mu\text{m}$  at 4.2 K, a) NMOS transistor output characteristic, b) PMOS transistor output characteristic.

effects and a hysteresis occur while sweeping  $V_{DS}$  from low to high voltages or in reverse direction. At liquid helium temperatures, the substrate becomes an insulator due to the freeze-out of ionized carriers. For sufficiently high drain-source voltages, holes are generated in the pinchoff region by weak avalanche generation. This charge cannot flow into the substrate, but remains under the gate and causes a threshold voltage shift, the so-called kink effect. The observed hysteresis can also be explained with the different possible recombination and conduction mechanisms [10]. As can be seen in Fig. 5(a) the output conductance of the n-channel transistor is partially negative if sweeping  $V_{DS}$  from high to low voltages. To overcome these device problems, mostly p-channel transistors are used in the amplifier design (p-channel transistors show a much weaker kink effect), and the operating points and the transistor dimensions are chosen to avoid the kink effects.

Beside these nonidealities, there is a remarkable change in the technology parameters. For instance, the channel mobility increases to  $\mu_n = 0.496 \text{ m}^2/\text{V}$  and  $\mu_p = 0.078 \text{ m}^2/\text{V}$  respectively, and the threshold voltage increases unsymmetrically to 1.25 V and  $-2.01 \text{ V}$  at 4.2 K. The sheet resistances for polysilicon,  $n^+$ - and  $p^+$ -diffusion layers decrease moderately at 4.2 K, whereas the substrate and p-well resistance increase dramatically due to carrier freeze-out. The junction capacitances decrease due to larger depletion regions, and also the subthreshold current coefficient at liquid helium decreases

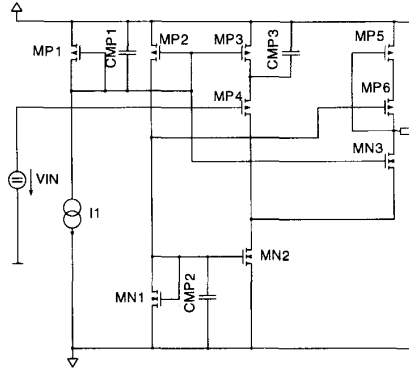


Fig. 6. Circuit diagram of the folded cascode preamplifier.

at least by a factor of 7. In particular, the high threshold voltages of the p-channel transistors makes a 5 V design more complicated.

#### IV. PREAMPLIFIER CIRCUIT

Due to the small input amplitude ( $< 100 \mu\text{V}$ ) and low linearity requirements of the preamplifier, an open loop configuration has been chosen. Moreover, the characteristic of the SQUID devices is also not highly linear. Fig. 6 shows the circuit diagram of the single-ended input folded cascode preamplifier. A nondifferential structure has been selected, since in this biomedical application, there are no specific power supply rejection ratio (PSRR) requirements. Since the folded cascode structure has only a high impedance node at the output, this structure features a high-gain bandwidth product. In Fig. 6,  $MP4$  is the input transistor,  $MN3$  forms the cascode transistor, and  $MP5$  and  $MP6$  are the load transistors. The folded cascode structure prevents the circuit from displaying kink effects. The biasing is accomplished with an external current source  $I1$  and current mirrors comprising transistors  $MP1$ ,  $MP2$ ,  $MP3$ , and  $MN1$ ,  $MN2$ . To stabilize the dc operating point, the quiescent current is mirrored from the current source into the driver transistor  $MP4$ . In the equivalent small signal network, transistor  $MP3$  can be substituted by a resistor. This resistor must be bypassed by a large external capacitor  $CMP3$  (1 nF), to ensure a common-source operation of transistor  $MP4$ . Since the capacitor is selected to provide a low impedance for the frequency band of interest, the frequency response of the amplifier has a bandpass characteristic. Neglecting the conductance of transistor  $MP4$ , the lower cut-off frequency is approximately defined by

$$\omega_L \cong \frac{g_{DS,MP3}}{C_{MP3}}. \quad (3)$$

In the interesting frequency range, the gate-source voltage of the input transistor equals the positive supply voltage  $V_{DD}$ .

To achieve the required high-noise performance, the input transistor  $MP4$  is made rather large ( $W/L = 1000 \mu\text{m}/2 \mu\text{m}$ ). The resistive poly-gate noise [11] is minimized by using a finger structure with 20 identical poly stripes. Both sides of the stripes are connected with aluminum. The substrate resistance noise [11], which modulates the channel current via the bulk transconductance  $g_{mb,MP4}$ , is kept as small as possible by surrounding the 20 individual transistors with a substrate contact ring with minimal distance.

In order to make the input transistor the dominant noise source, the noise contribution of the current source  $MN2$  and the output load (transistors  $MP5$  and  $MP6$ ) has to be kept negligibly smaller. The noise contribution of the cascode transistor is always negligible as the result of the strong source degeneration effect due to high output impedance of the input transistor [11]. By choosing a channel length of  $5 \mu\text{m}$  and a relatively high effective gate-source voltage of transistors  $MN2$  and  $MP6$ , their noise contribution can be neglected. The output resistance is decreased by the feedback connected gate of  $MP5$ . The output resistance is given [see (4) at bottom of page]. Contrary to the usual cascode load, where the resistance is approximately  $\{g_{m,MP6}/g_{DS,MP6} * g_{DS,MP5}\}$  the output resistance is given by (4). This feedback connection and the other design provisions ensure that the noise of the input transistor  $MP4$  is the dominant noise. In addition, the low output resistance linearizes the dc transfer function by limiting the signal swing (the overall gain in the frequency range of interest is limited to a factor of 16).

The folded cascode structure and especially, the cascode load, prevents the output transistors from working in ranges where the kink effect occurs by limiting the drain-source voltage of each output transistor. Each transistor is surrounded by a substrate or a well contact ring, which collects injected charges under the gates of the transistors and prevents kink effects. Fig. 7 depicts the photomicrograph of the amplifier.

#### V. EXPERIMENTAL RESULTS

The preamplifier is fabricated in a  $1 \mu\text{m}$  p-well CMOS technology and occupies an area of  $0.3 \text{ mm}^2$ . The external bias current was set to  $325 \mu\text{A}$ , so that the input transistor is biased with  $650 \mu\text{A}$ . The supply voltage was switched on before cooling the test circuits. Fig. 8 shows the input and output signal at the operating temperature of 4.2 K. During the measurements no abnormal behavior of the amplifier has been recognized. The measured gain at 300 KHz is about 24 dB for a power supply voltage of  $\pm 2.5 \text{ V}$ . The power consumption is 9 mW. The cut-off frequencies are 22 kHz and 308 kHz for a load of 600 pF. (This high value of capacitance is due to the long cable necessary for measurement in a 4 K environment). The measured frequency response is depicted in Fig. 9. For a capacity of 60 pF the higher cut-off frequency is ten times higher. The measured output resistance is 3 k $\Omega$ ,

$$R_{\text{out}} = \frac{(g_{m,MP6} + g_{mb,MP6} + g_{DS,MP6} + g_{DS,MP5})}{g_{m,MP5} * (g_{m,MP6} + g_{mb,MP6} + g_{DS,MP6}) + g_{DS,MP5} * g_{DS,MP6}} \cong \frac{1}{g_{m,MP5}} \quad (4)$$

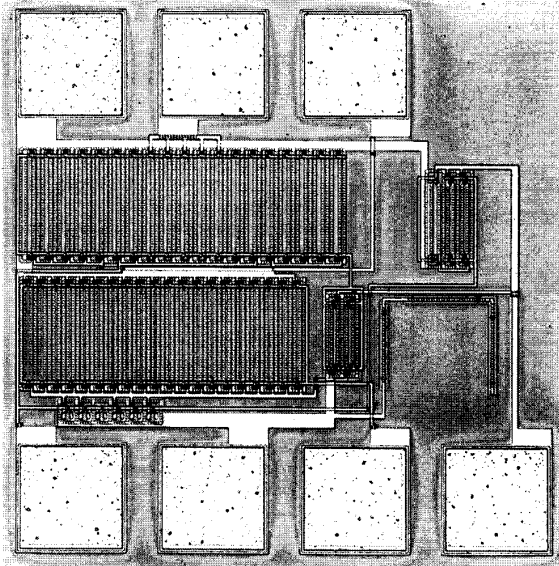


Fig. 7. Microphotograph of the preamplifier.

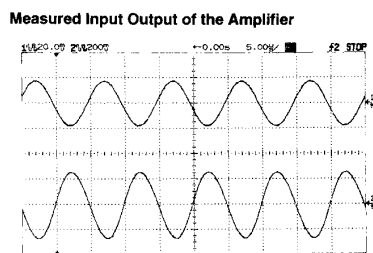


Fig. 8. Measured input and output of the amplifier.

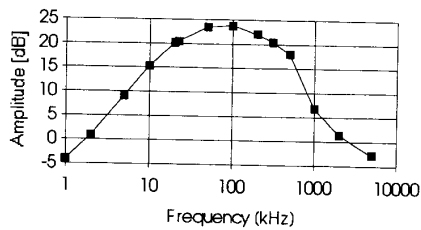


Fig. 9. Measured frequency response of the amplifier.

and the measured equivalent input noise density is shown in Fig. 10. As can be seen from the figure the  $1/f$  noise is dominant. It is approximately a factor 3 greater than its value at 300 K. The performance data of the preamplifier are summarized in Table I.

## VI. CONCLUSION

An integrated CMOS preamplifier for biomagnetic applications has been presented, which operates at 4 K. No unusual

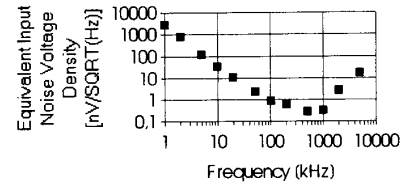


Fig. 10. Measured equivalent input noise voltage density.

TABLE I  
PERFORMANCE DATA OF THE PREAMPLIFIER

Operating Temperature	4.2 K
Power Supply Voltage	+2.5 V; -2.5 V
Gain (300 kHz)	24 dB
Output Swing	400 mV
Bandwidth ( $C_L = 600$ pF)	22 kHz–308 kHz
Equivalent Input Noise Density (300 kHz)	0.3 nV/√Hz
Output Resistance	3 kΩ
Power Consumption ( $V_{DD} = 5$ V)	9 mW
Chip Area	0.3 mm <sup>2</sup>

behavior of the amplifier at liquid helium temperatures has been observed. The input of the amplifier can be connected directly to a SQUID output. As a result, the series resonant tank circuit is no longer required and the flux locked loop has a much greater bandwidth than in the previous system. The measured equivalent input noise of the preamplifier is less than 0.5 nV/√Hz in the frequency range of interest. With the help of such a preamplifier circuit the expensive shielding can be simplified.

## ACKNOWLEDGMENT

The authors wish to thank M. Zedler for measuring the transistor characteristics at 4 K and M. Bollu for evaluating the corresponding technology parameters.

## REFERENCES

- [1] H. E. Hoenig, G. Daalmans, W. Folberth, H. Reichenberger, S. Schneider, and H. Seifert, "Biomagnetic multichannel system with integrated SQUIDs and first order gradiometers operating in a shielded room," *Cryogenics*, vol. 29, pp. 809–813, Aug. 1989.
- [2] S. Schneider, H. Seifert, H. E. Hoenig, and H. Reichenberger, "Design and operation of a biomagnetic multichannel system," in *Springer Proceedings in Physics*, vol. 64: *Superconducting Devices and Their Applications*, H. Koch and H. Lübbig, Eds. Berlin: Springer-Verlag, 1992.
- [3] T. Van Duzer and C. W. Turner, *Principles of Superconductive Devices and Circuits*, New York: Elsevier North-Holland, 1981.
- [4] T. Ryhänen, H. Seppä, R. Ilmoniemi, and J. Knuutila, "SQUID magnetometers for low-frequency applications," *J. Low Temperature Physics*, vol. 76, nos. 5/6, pp. 287–386, 1989.
- [5] B. D. Josephson, "Possible new effects in superconductive tunneling," *Phys. Lett.*, vol. 1, pp. 251–253, July 1962.
- [6] J. Clarke, W. M. Goubau, and M. B. Ketchen, *J. Low. Temp. Phys.*, vol. 25, p. 95, 1978.
- [7] R. Cantor, D. Drung, M. Peters, H. J. Scheer, and H. Koch, "Integrated DC SQUID magnetometer with simplified read-out," *Supercond. Sci. Technol.* 3, pp. 108–112, 1990.
- [8] S. K. Tewksbury, "N-channel enhancement-mode MOSFET characteristic from 10 to 300 K," *IEEE Trans. Electron Devices*, vol. 28, pp. 1519–1529, Dec. 1981.
- [9] H. Hanamura, M. Aoki, T. Masuhara, O. Minato, Y. Sakai, and T. Hayashida, "Operation of bulk CMOS devices at very low temperatures," *IEEE J. Solid-State Circuits*, vol. 21, no. 3, pp. 484–490, June 1986.

- [10] B. Dierickx, L. Warmerdam, E. Simeon, J. Vermeiren, and C. Claeys, "Model for hysteresis and kink behavior of CMOS transistors operating at 4.2 K," *IEEE Electron Devices*, vol. 35, no. 7, pp. 1120-1125, July 1988.
- [11] Z. Y. Chang and W. M. C. Sansen, "Low-noise wide-band amplifiers in bipolar and CMOS technologies," Kluwer Academic, 1991.



**Ulrich Kleine** (M'81) was born in Hagen, Germany, on February 14, 1954. He received the Dipl.-Ing. degree and the Dr.-Ing. degree from the University of Dortmund, Germany, in 1979 and 1985, respectively.

From 1980 to 1984 he had been with the Lehrstuhl Bauelemente der Elektrotechnik, Department of Electrical Engineering, University of Dortmund, where he worked on linear and nonlinear switched capacitor networks, especially on wave SC filters. Since January 1985 he has been with the

Corporate Research and Development Laboratories of the Siemens AG in Munich, working in the field of analog and digital signal processing hardware and design automation.



**Johannes Bieger** was born in Nuremberg, Germany, on December 27, 1952. He received the Dipl.Phys. degree and the Dr.rer.nat. degree from the University of Erlangen, Erlangen, Germany, in 1977 and 1983, respectively.

From 1983 to 1988, he had been with the Central Research Laboratories of Siemens AG in Munich, where he worked on integrated circuits process development. Since October 1988, he has been with Siemens AG Medical Engineering Group in Erlangen, working on biomagnetism and on therapeutic ultrasound.



**Heinrich Seifert** was born in Nanded, Germany, on May 27, 1950. He received the Dipl.Phys. degree from the University of Karlsruhe, Germany, in 1976, and the Dr.rer.nat. degree from the University of Tuebingen, Tuebingen, Germany, in 1981.

He worked until 1985 on nonequilibrium and Josephson effects in superconductors at the University of Tuebingen. From 1985 to 1990, he has been with the Central Research Laboratories, and since 1990, with the Medical Engineering Group of the Siemens AG in Erlangen, Germany, working on biomagnetism.